ACTA TECHNICA CORVINIENSIS – Bulletin of Engineering | e–ISSN: 2067 – 3809
Tome XVII [2024] | Fascicule 2 [April – June]

[1.] Muharrem Hilmi AKSOY, [2.] Ali ÖNER, [1.] Muhammed Osman DUMAN, [1.] Mert TURAN

NUMERICAL ANALYSIS OF GAS–SOLID FLOW IN A REVERSE FLOW CYCLONE SEPARATOR

[1.] Konya Technical University, Faculty of Engineering and Natural Science, Department of Mechanical Engineering, Konya, TÜRKIYE
[2.] İmaş Machinery Inc. R&D Center, Konya, TÜRKIYE

Abstract: Aerocyclone separators are crucial in separating solid particles from gas streams. These cyclones exhibit diverse geometrical configurations in their inlet zones, including tangential, spiral, helical, and axial designs, with variations within the tangential type. Beyond their economic appeal, these devices are characterized by their resilience to high temperatures and pressures, ease of manufacturing, and uncomplicated geometrical structures. Among the factors influencing cyclone performance, the critical parameters of interest encompass dust collection efficiency and pressure loss. The present study employed a Stairmand–type counter–flow cyclone to separate flour particles dispersed within an air medium. A numerical investigation considered cyclone heights of H = 750 mm, H = 1000 mm, and H = 1500 mm. Furthermore, cyclone inlet velocities of 8 m/s, 13 m/s, and 17 m/s were specifically chosen for examination. Particle sizes ranged from 1 to 10 micrometers, ensuring the evaluation extended to conditions achieving 100% collection efficiency. A comprehensive analysis of pressure drop ratios was presented herein, offering insights into the impact of varying inlet speeds and cyclone dimensions.

Keywords: cyclone, collection efficiency, pressure drop, flow analysis

INTRODUCTION

The separation of gases and the solid particles they carry is important in process industries, and it is achieved through various methods. Solid particles can intentionally be present in the gas flow, for example, in pneumatic conveying systems, where it may be necessary for 100% solid recovery at the end of the conveying process to have an economical process [1–2]. The applied centrifugal force forms a vortex inside the cyclone, and the gas swirls toward the conical bottom. Larger particles with a considerable diameter are then pushed towards the wall and separated from the gas. In the conical section, the gas flow reverses direction to move upward over the central part of the cyclone and exits from the top through the gas outlet pipe. Meanwhile, solid particles move downward along the wall and accumulate at the bottom of the conical section [3–4].

Cyclone separators are widely used in industries to separate and collect particles from gases or similar gas mixtures containing solid particles such as dust, chips, or grains. They are used in industrial dust collection systems to capture particles as small as 50 microns. Commercial cyclones can operate at flow rates ranging from 50 to 5000 m3/h. In cases where they do not provide the required efficiency, they can be used in conjunction with high–efficiency collection devices. Cyclone separators are categorized into two groups: axial inlet cyclones and tangential inlet cyclones [5–6]

Shepperd & Lapple, Avant, Parnell & Sorenson cyclone models are commonly used in the agricultural industry. Simpson & Parnell, to address the cotton processing sector's lint problem, used a low–pressure cyclone model. The Stairmand Cyclone was selected in this study due to its high dust collection efficiency [7].

Several parameters influence cyclone performance. These parameters include the type of cyclone, cyclone dimensional ratios, outlet pipe height (stack), cyclone inlet velocity, outlet pipe diameter, temperature, and variations in particle concentration. Altering these parameters can affect cyclone performance criteria, such as pressure drop and efficiency [8].

The literature review comprehensively examines research endeavors focused on comprehending and optimizing cyclone separator performance. Scholars have rigorously investigated the impact of diverse factors such as geometry, flow rates, and particle concentration on cyclone efficiency and pressure drops. Pioneering work by Leith and Licht [9] introduced a theory for calculating particle collection efficiency in cyclone separators, incorporating the drag coefficient to enhance particle collection efficiency. Their efforts also yielded an efficiency model capable of accounting for pressure losses. Subsequent studies, like those by Griffiths and Boysan [10], employed numerical simulations to analyze particle capture efficiency and pressure drops in different cyclones, aligning their findings with existing literature. Barth's [11] model was found accurate for small cyclones, whereas lozia

and Leith's [12] model proved precise for larger counterparts. The integration of CFD analyses further enriched the field, providing reliable predictions for pressure drops and particle capture efficiency. Bohnet [13] delved into experimental studies, examining cyclone performance at high temperatures, revealing significant pressure drops and efficiency curves for specific temperature values. Linden and Gudmundsson [14] explored parameters affecting cyclone collection efficiency, highlighting the critical influence of the ratio of cyclone body diameter to vortex tube inner diameter and its independence from the Reynolds number.

Avcı and Erel [15] introduced an approach to determine optimal cyclone length, finding no efficiency increase beyond a certain length, suggesting potential adjustments at high and low velocities. Avcı and Karagöz [16] explored the effects of flow and geometric parameters, unveiling the significant roles of surface friction, vortex length, and flow regime. Faulkner et al. [17] identified an inverse relationship between cyclone diameter and efficiency. Advanced computational techniques, as evidenced by Kaya and Karagöz [18], emphasized the accuracy of the Reynolds turbulence model in predicting cyclone behavior. Novel designs, like Tan F.'s [19] modified cyclone, showcased the potential for reimagining cyclone structures. Erol et al. [20] employed numerical and experimental methods, refining our understanding of exit pipe diameter influence. Recent studies, including those by Chu et al. [21], Pandey and Brar [22], and El–Emam et al. [23], harnessed advanced computational and experimental techniques, pushing the boundaries of cyclone optimization.

In this study, a Stairmand–type counter–flow cyclone was used to separate flour particles in an air medium. Numerical simulations were conducted with cyclone heights of 750 mm, 1000 mm, and 1500 mm, along with inlet velocities of 8 m/s, 13 m/s, and 17 m/s. Particle sizes ranged from 1 to 10 micrometers, allowing for a thorough evaluation of conditions and achieving 100% collection efficiency. The analysis included a detailed examination of pressure drop ratios, providing valuable insights into the effects of different speeds and cyclone dimensions.

MATERIAL AND METHODS

In the study, the particle bulk density was assumed to be 550 kg/m³, and a flow rate of 1000 m³/h of air contained 18 kg of these particles. Two distinct groups of parameters are employed in the design of aerosol cyclones. This study focuses on parameters based on design, which vary according to the selected cyclone type. The selection and manipulation of these parameters play a pivotal role in the design and performance optimization of aerosol cyclones. Different cyclone types require adjustments in these parameters to achieve desired efficiency and particle separation outcomes. Figure 1 presents the design parameters specific to the Stairmand–type cyclone. These parameters are integral to the intricate process of cyclone design. In Stairmand–type cyclones, the parameters are dimensioned relative to the body diameter "D" [24].

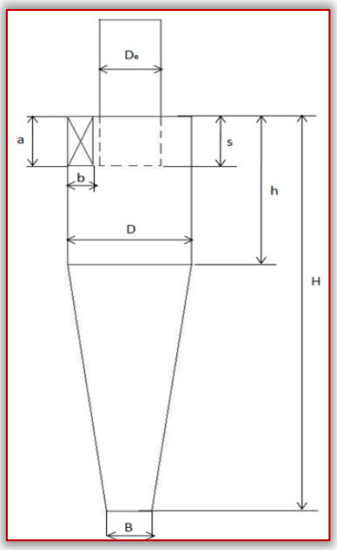

Figure 1. The design parameters of the Stairmand type cyclone

Table 1. The dimensions of the Stairmand cyclone

Parameter	Dimension*D
Cyclone diameter, D	1.0 D
Air outlet pipe diameter, De	0.5 D
Height of air inlet section, a	0.5 D
Width of air inlet section, b	0.2 D
Dip depth of the outlet pipe, s	0.5 D
Cyclone height, H	4.0 D
Body height, h	1.5 D
Dust outlet diameter, B	0.375 D

When multiplied by the body diameter "D", these standardized dimensions provide precise measurements for each component, ensuring consistency and accuracy in the design and evaluation of Stairmand–type cyclones.

In the computational fluid dynamics (CFD) analysis, parameters were meticulously chosen to simulate the complex dynamics within the cyclone separator. Particle density was fixed at 0.80 kg/m3 for flour material. The simulation's choice of spherical particle shape was made to capture real–world scenarios accurately. The gas flowing into the system was at a stable

temperature of 27 °C, with an outlet pressure maintained at 101625 Pa. Furthermore, the air density was chosen as air set at 1.1 kg/m^3, while the viscosity was calculated at 1.7810^{-5} kg/(ms). The ambient temperature was also held constant at 27°C, reflecting standard environmental conditions. The inlet velocities, a critical variable influencing the cyclone's efficiency, were tested at three different values: 8 m/s, 13 m/s, and 17 m/s. This range allowed for a comprehensive analysis of the cyclone's performance under various flow rates, providing valuable insights into its operational flexibility. Moreover, the surface roughness of the cyclone material was specified at 0.39, a factor contributing significantly to the friction between particles and the cyclone walls as taken as a metal sheet. These chosen parameters served as the foundation for the computational analysis, enabling a detailed exploration of the cyclone separator's behavior under different operating conditions.

The K–Epsilon Model has been a foundational tool for simulating turbulent flows in CFD. A modification called the RNG Option was introduced to enhance accuracy in swirling flows. Specifically tailored for swirl–dominated scenarios, this adjustment ensures precise simulations by employing standard wall functions for near–wall treatment. For the CFD analysis, specific boundary conditions are set:

Inlet and Wall: Particles rebound off these boundaries, with their momentum changing as determined by the coefficient of restitution. Outlet (Top): When particles encounter this boundary, their trajectories end, signifying that they have 'escaped.' Outlet (Bottom/Dustbin): Particle trajectories are terminated, and the outcome is recorded as 'trapped.' For evaporating droplets, their entire mass instantly transitions into the adjacent cell's vapor phase. In the case of a combusting particle, the remaining volatile mass enters the vapor phase.

In the realm of CFD analysis, the concept of separation efficiency in cyclone separators is crucial. It quantifies the fraction of particles of a specific size captured within the cyclone concerning those particles of the same size entering the cyclone. Empirical observations have demonstrated that the efficiency of cyclone separators rises with increasing particle mean diameter and density, heightened gas tangential velocity, diminished cyclone diameter, elongated cyclone length, and the removal of gas alongside solids through the cyclone legs. In this context, the Separation Efficiency is precisely defined based on particle history data. It represents the proportion of concentration removed from the incoming feed stream compared to the initial concentration. This efficiency measure is calculated by determining the ratio of trapped particles to the total number of particles tracked in the system, as given in Eq 1.

$$\text{Efficieny} = \frac{\text{N. of particles trapped}}{\text{N. of particles tracked}} \quad (1)$$

In practical engineering applications, derivatives of the k–ε model exhibit comparable structures, featuring transport equations for turbulent kinetic energy (k) and dissipation rate (ε). The Renormalization Group (RNG) k–ε model is grounded in the instantaneous Navier–Stokes equations. It sets the RNG k–ε model apart from the Standard k–ε model is analytical derivation, involving incorporating model constants and supplementary terms within the transport equations [25].

$$\frac{\partial}{\partial t}(\rho k) + \frac{\partial}{\partial x_i}(\rho k u_i) = \frac{\partial}{\partial x_i}\left[\mu_{eff}\alpha_k \frac{\partial k}{\partial x_j}\right] + G_k - \rho\varepsilon + S_k \quad (2)$$

$$\frac{\partial}{\partial t}(\rho\varepsilon) + \frac{\partial}{\partial x_i}(\rho\varepsilon u_i) = \frac{\partial}{\partial x_i}\left[\mu_{eff}\alpha_k \frac{\partial \varepsilon}{\partial x_j}\right] + C_{1\varepsilon}G_k\frac{\varepsilon}{k} - C_{2\varepsilon}\rho\frac{\varepsilon^2}{k} - R_\varepsilon + S_\varepsilon \quad (3)$$

The fundamental disparity between the RNG (Renormalization Group) and the standard k–ε turbulence models lies in the presence of an additional term within the dissipation rate (ε) equation, depicted as follows:

$$R_\varepsilon = \frac{C_\mu \rho \eta^3 (1 - \eta/\eta_0)}{1 + \beta\eta^3}\frac{\varepsilon^2}{k} \quad (4)$$

In this equation, the constant Cμ is set to 0.0845, η≡Sk/ε, η_0 equals 4.38, and β equals 0.012. Notably, the RNG model exhibits heightened sensitivity to strain and streamline curvature impacts when contrasted with the Standard k–ε model, where the constants C1ε and C2ε are 1.44 and 1.92, respectively.

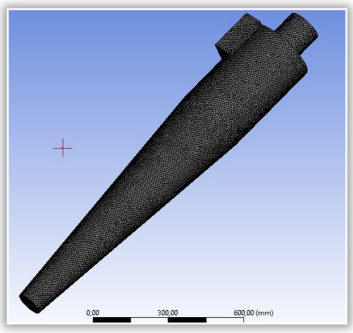

Figure 2. Mesh structure of the cyclone

A mesh independency study indicates that 4x10^5, 9,5x10^5, and 20x10^5 elements are deemed

adequate for 750 mm, 1000 mm, and 1500 mm for the analyses, respectively. A mesh structure used in this study is given in Fig.2.

RESULTS AND DISCUSSION

In the following section, we delve into the results and discussions derived from CFD analysis of cyclone separators. Through the computational simulations, we have explored various parameters that significantly influence cyclone performance, including geometry modifications and flow rates. Tangential and axial velocities are important factors for the particle collection in the cyclones. The total pressure contours in Figures 3, 4, and 5 are presented at inlet velocities of 8, 13, and 17 m/s, respectively. These figures illustrate pressure variations in three dimensions, corresponding to different H heights, denoted as options a, b, and c. Geometric measurements have been adjusted to represent diverse pressure changes in these three–dimensional contexts. Due to swirling velocity within the cyclone, a distinct negative pressure zone manifests in its central region. Remarkably, the pressure reaches its nadir close to the cyclone's center, contrasting sharply with the positive and maximal pressure values observed near the cyclone periphery. This signifies a radial decline in pressure, where the pressure diminishes from the wall towards the core. Notably, as the diameter of the vortex finder decreases, there is a discernible augmentation in pressure. This phenomenon underscores the significant correlation between pressure and velocity. Consequently, an escalation in tangential velocity is anticipated to correspond with an elevation in pressure. Furthermore, the study observes a substantial pressure gradient along the radial direction, emphasizing its pronounced nature in this dimension, while it remains comparatively restricted in the axial orientation. This intricate interplay between velocity, pressure, and geometry underscores the complex dynamics at play within cyclonic systems.

In cyclone design, paramount objectives are maximizing separation efficiency while minimizing pressure drop. A superior separation efficiency and a minimal pressure drop constitute the optimal outcome for cyclone designs. This intricate balance necessitates understanding various physical and geometrical variables that influence cyclone behavior. These variables encompass particle density, gas viscosity, cyclone dimensions, particle cut–off diameter, inlet velocity, and numerous other factors.

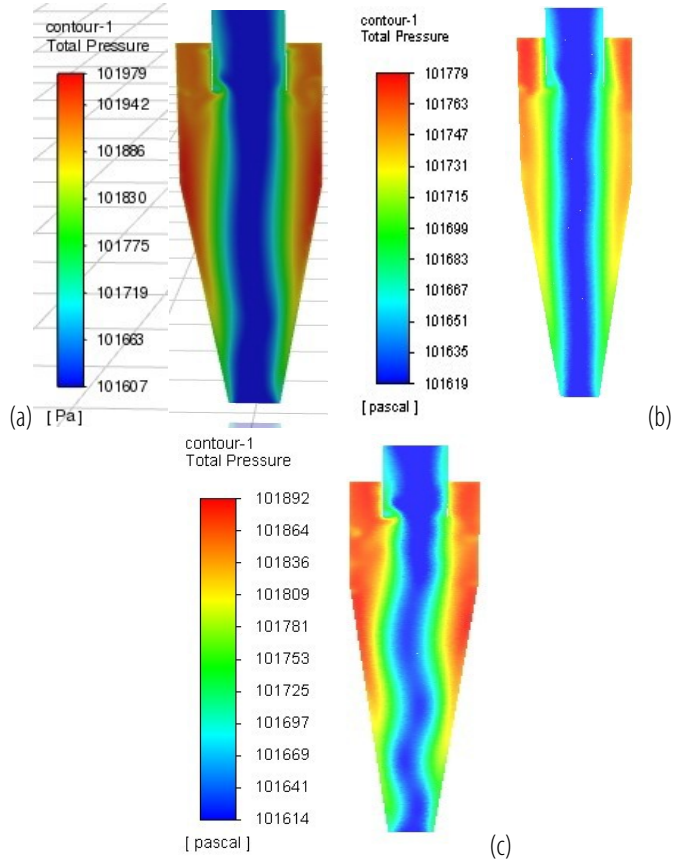

Figure 3. Pressure Contours in Cyclones with (a) H = 750 mm, (b) H = 1000 mm, and (c) H = 1500 mm at a Velocity of 8 m/s.

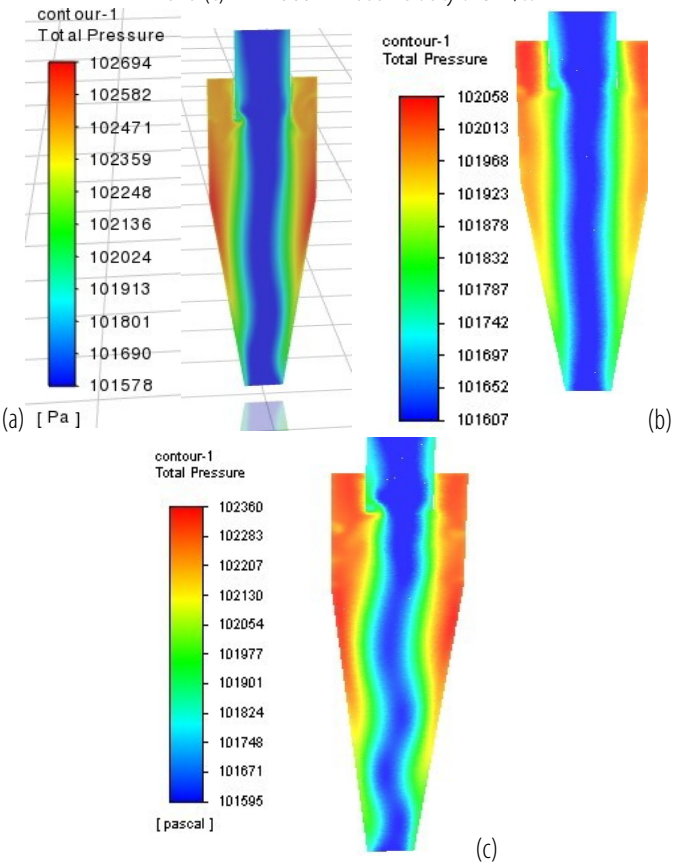

Figure 4. Pressure Contours in Cyclones with (a) H = 750 mm, (b) H = 1000 mm, and (c) H = 1500 mm at a Velocity of 13 m/s.

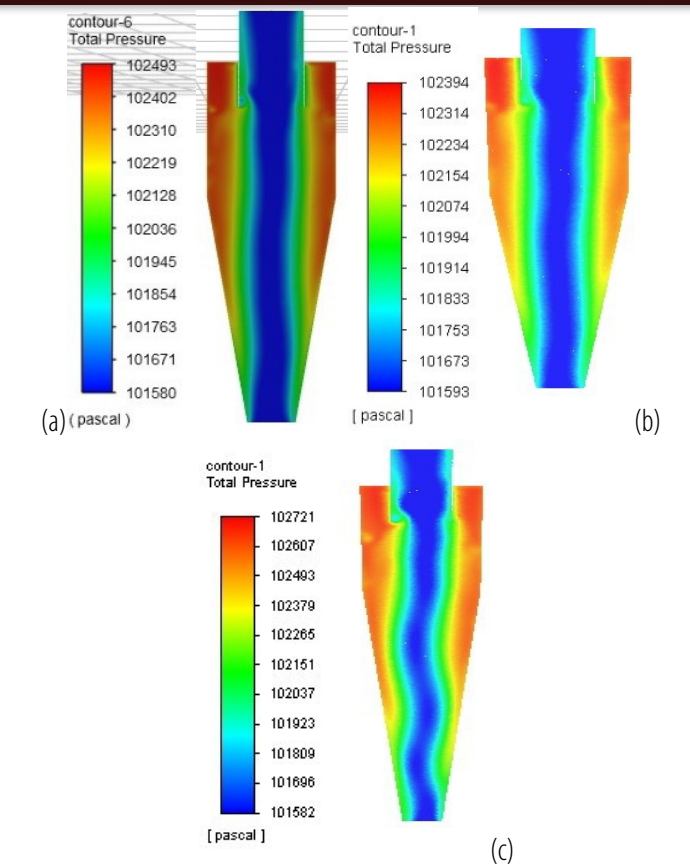

Figure 5. Pressure Contours in Cyclones with (a) H = 750 mm, (b) H = 1000 mm, and (c) H = 1500 mm at a Velocity of 17 m/s.

The manipulation and comprehension of these variables are pivotal in crafting cyclone designs that align with the desired efficiency and pressure drop criteria, reflecting the intricate interplay of diverse parameters in cyclone performance optimization. The impact of inlet velocity on fractional separation efficiency is a critical aspect of cyclone separator performance analysis. Understanding how varying inlet velocities influence particle separation efficiency is essential for optimizing cyclone designs. This parameter significantly affects the cyclone's ability to capture particles of different sizes and densities, directly influencing the separation process's overall efficiency.

In the discrete phase model, particles are introduced at the cyclone's inlet and meticulously tracked to assess fractional separation efficiency, a crucial parameter in cyclone performance evaluation. The separation efficiency represents the ratio of captured particles to those injected, considering incomplete particles. Particles ranging from 1 to 10 μm diameter were released at the inlet to simulate the cyclone's separation efficiency. Figure 6 illustrates the separation efficiency concerning particle diameter at three distinct inlet velocities for a cyclone with different diameters. The graph depicts a direct correlation between efficiency, particle size, and inlet velocity, indicating that higher efficiencies are achieved with larger particles and increased inlet velocities. This relationship is rooted in the proportional nature of centrifugal force to flow velocity, highlighting the direct influence of centrifugal force on collection efficiency. As it is seen, as the H height increases, 100% efficiency is achieved at higher particle size.

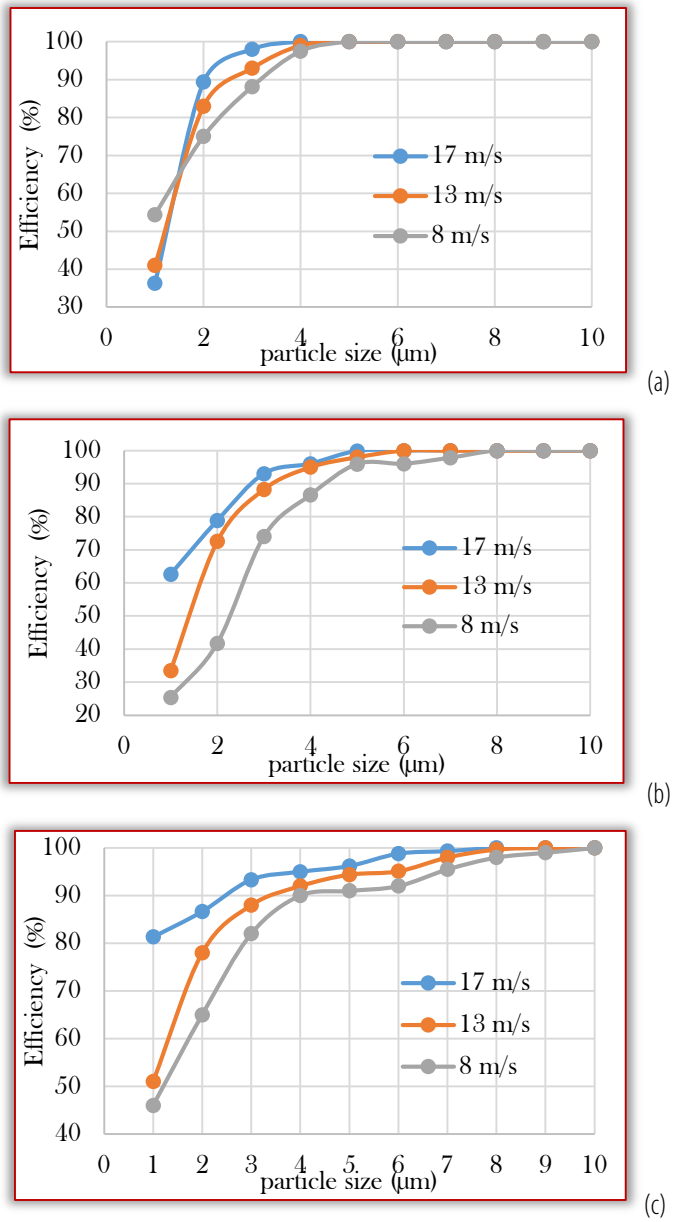

Figure 6. The effect of the inlet velocity on separation efficiency of cyclones (a) H = 750 mm, (b) H = 1000 mm, and (c) H = 1500 mm

CONCLUSION

In this comprehensive study, the intricate dynamics of cyclone separators were meticulously explored through CFD simulations. The focus was on a Stairmand–type counter–flow cyclone utilized for separating flour particles within an air medium. The research delved into an array of crucial parameters, including cyclone heights (H = 750 mm, H = 1000 mm, and

H = 1500 mm) and inlet velocities (8 m/s, 13 m/s, and 17 m/s). This systematic analysis provided deep insights into the cyclone's behavior under diverse operational conditions.

One of the key findings highlighted the significant influence of geometry and flow rates on cyclone performance. The analysis of pressure contours revealed intricate patterns within the cyclone structure. A notable negative pressure zone was observed in the central region due to swirling velocity, with pressure reaching its minimum at the cyclone's center. This was sharply contrasted by positive and maximal pressure values near the cyclone periphery, illustrating a radial decline in pressure from the wall toward the core. Moreover, the reduction in the vortex finder diameter increased pressure, emphasizing the direct correlation between pressure and velocity.

In examining the impact of inlet velocity on fractional separation efficiency, a critical aspect of cyclone performance, the study revealed a direct relationship between efficiency, particle size, and inlet velocity. Larger particles and increased inlet velocities resulted in higher efficiencies, underlining the pivotal role of centrifugal force proportional to flow velocity in the collection process.

Future research directions could delve deeper into integrating advanced materials on surfaces, optimized geometries, and experimental techniques to enhance cyclone separator efficiency further and contribute to sustainable industrial practices in milling and other industries.

References

[1] Jüttner, K., U. Galla, and H. Schmieder. "Electrochemical approaches to environmental problems in the process industry." Electrochimica Acta 45.15–16 (2000): 2575–2594.
[2] Utikar, Ranjeet, et al. "Hydrodynamic simulation of cyclone separators." Computational fluid dynamics. InTech, 2010. 241–266.
[3] Wang, B., Xu, D. L., Chu, K. W., & Yu, A. B. (2006). Numerical study of gas–solid flow in a cyclone separator. Applied Mathematical Modelling, 30(11), 1326–1342.
[4] Liu, Z., Zheng, Y., Jia, L., Jiao, J., & Zhang, Q. (2006). Stereoscopic PIV studies on the swirling flow structure in a gas cyclone. Chemical Engineering Science, 61(13), 4252–4261.
[5] Obernberger, I., Brunner, T., & Bärnthaler, G. (2006). Chemical properties of solid biofuels—significance and impact. Biomass and bioenergy, 30(11), 973–982.
[6] Schummer, P., Noe, P., & Baker, M. (1992). LDV measurements in the vortex flow created by a rotating wall dewatering cyclone. In Hydrocyclones: Analysis and Applications (pp. 359–376). Dordrecht: Springer Netherlands.
[7] Sharma, G., & Majdalani, J. (2022). Effects of various inlet parameters on the computed flow development in a bidirectional vortex chamber. Physics of Fluids, 34(4).
[8] Bhasker, C. (2010). Flow simulation in industrial cyclone separator. Advances in Engineering software, 41(2), 220–228.
[9] Leith , D. , and Licht , W. (1972). AIChE Sym. Ser. 68 : 196
[10] Griffiths, W. D., & Boysan, F. (1996). Computational fluid dynamics (CFD) and empirical modelling of the performance of a number of cyclone samplers. Journal of Aerosol Science, 27(2), 281–304.
[11] Barth, W. (1956). Berechnung und auslegung von zyklonabscheidern auf grund neuer untersuchungen. Brennst.–Warme–Kraft, 8, 1–9.
[12] Iozia, D. L., & Leith, D. (1989). Effect of cyclone dimensions on gas flow pattern and collection efficiency. Aerosol Science and Technology, 10(3), 491–500.
[13] Bohnet, M., Gottschalk, O., & Morweiser, M. (1997). Modern design of aerocyclones. Advanced Powder Technology, 8(2), 137–161.
[14] Lidén, G., & Gudmundsson, A. (1997). Semi–empirical modelling to generalise the dependence of cyclone collection efficiency on operating conditions and cyclone design. Journal of aerosol science, 28(5), 853–874.
[15] Avcı, A., & Erel, G. K. (2003). Siklon separatörlerde uzunluğun verime etkisi ve optimizasyonu. Uludağ Üniversitesi Mühendislik–Mimarlık Fakültesi Dergisi, 8(1), 101–109.
[16] Karagoz, I., & Avci, A. (2005). Modelling of the pressure drop in tangential inlet cyclone separators. Aerosol Science and Technology, 39(9), 857–865.
[17] Faulkner, W. B., Buser, M. D., Whitelock, D. P., & Shaw, B. W. (2008). Effects of cyclone diameter on performance of 1D3D cyclones: cutpoint and slope. Transactions of the ASABE, 51(1), 287–292.
[18] Kaya, F., & Karagoz, I. J. C. E. (2008). Performance analysis of numerical schemes in highly swirling turbulent flows in cyclones. Current science, 1273–1278.
[19] Tan, F., Karagoz, I., & Avci, A. (2016). Effects of geometrical parameters on the pressure drop for a modified cyclone separator. Chemical Engineering & Technology, 39(3), 576–581.
[20] Erol, H. I., Turgut, O., & Unal, R. (2019). Experimental and numerical study of Stairmand cyclone separators: a comparison of the results of small–scale and large–scale cyclones. Heat and Mass Transfer, 55, 2341–2354.
[21] Chu, K., Chen, Y., Ji, L., Zhou, Z., Yu, A., & Chen, J. (2022). Coarse–grained CFD–DEM study of Gas–solid flow in gas cyclone. Chemical Engineering Science, 260, 117906.
[22] Pandey, S., & Brar, L. S. (2022). On the performance of cyclone separators with different shapes of the conical section using CFD. Powder Technology, 407, 117629.
[23] El–Emam, M. A., Zhou, L., & Omara, A. I. (2023). Predicting the performance of aero–type cyclone separators with different spiral inlets under macroscopic bio–granular flow using CFD–DEM modelling. Biosystems Engineering, 233, 125–150.
[24] Brar, L. S., Sharma, R. P., & Elsayed, K. (2015). The effect of the cyclone length on the performance of Stairmand high–efficiency cyclone. Powder Technology, 286, 668–677.
[25] Shaheed, R., Mohammadian, A., & Kheirkhah Gildeh, H. (2019). A comparison of standard k–ε and realizable k–ε turbulence models in curved and confluent channels. Environmental Fluid Mechanics, 19, 543–568.

Note: This paper was presented at IIZS 2023 – The XIII International Conference on Industrial Engineering and Environmental Protection, organized by Department of Mechanical Engineering and Department of Environmental Protection of the Technical Faculty "Mihajlo Pupin" Zrenjanin, from the University of Novi Sad, in cooperation with partners – University Politehnica Timisoara, Faculty of Engineering, Hunedoara (ROMANIA), University "St. Kliment Ohridski", Technical Faculty, Bitola (MACEDONIA), "Aurel Vlaicu" University of Arad, Faculty Of Engineering, Arad (ROMANIA), University of East Sarajevo, Faculty of Mechanical Engineering East Sarajevo, Sarajevo (BOSNIA & HERZEGOVINA) and University of Giresun, Faculty of Engineering, Giresun (TURKEY) – in Zrenjanin, SERBIA, in 05–06 October, 2023.

ISSN: 2067–3809